Intracellular calcium signals measured with indo-1 in isolated skeletal muscle fibres from control and *mdx* mice

Claude Collet, Bruno Allard, Yves Tourneur and Vincent Jacquemond

Laboratoire de Physiologie des Eléments Excitables, CNRS UMR 5578, Université Claude Bernard Lyon 1, 43 boulevard du 11 Novembre 1918, 69622 Villeurbanne Cedex, France

(Received 6 April 1999; accepted after revision 3 August 1999)

1. Intracellular free calcium concentration ($[Ca^{2+}]_i$) was measured with the fluorescent indicator indo-1 in single skeletal fibres enzymatically isolated from the flexor digitorum brevis and interosseus muscles of control and dystrophic *mdx* C57BL/10 mice. Measurements were taken from a portion of fibre that was voltage clamped to allow detection of depolarization-induced changes in $[Ca^{2+}]_i$.

2. The mean (± S.E.M.) initial resting $[Ca^{2+}]_i$ from all control and *mdx* fibres tested was 56 ± 5 nM ($n = 72$) and 48 ± 7 nM ($n = 57$), respectively, indicating no significant overall difference between the two groups. However, when comparing a batch of control and *mdx* fibres obtained from mice older than ~35 weeks, resting $[Ca^{2+}]_i$ was significantly lower in *mdx* (16 ± 4 nM, $n = 11$) than in control fibres (71 ± 10 nM, $n = 14$).

3. Changes in $[Ca^{2+}]_i$ elicited by short (5–35 ms) depolarizing pulses from −80 to 0 mV showed similar properties in control and *mdx* fibres. After a 5 ms duration pulse the mean time constant of $[Ca^{2+}]_i$ decay was, however, significantly elevated in *mdx* as compared to control fibres, by a factor of 1·5–2. For longer pulses, no significant difference could be detected.

4. In response to 50 ms duration depolarizing pulses of various amplitudes the threshold for detection of an $[Ca^{2+}]_i$ change and the peak $[Ca^{2+}]_i$ reached for a given potential were similar in control and *mdx* fibres.

5. Overall results show that *mdx* skeletal muscle fibres are quite capable of handling $[Ca^{2+}]_i$ at rest and in response to membrane depolarizations.

Skeletal muscles from the *mdx* mouse lack dystrophin (Bulfield *et al.* 1984), a protein that is associated with the subsurface membrane cytoskeleton (Watkins *et al.* 1988; Berthier *et al.* 1995) and also with the transverse tubular membrane at the level of the triadic junction (Hoffman *et al.* 1987). The failure in dystrophin expression results from a genetic defect that is homologous to the one responsible for Duchenne muscular dystrophy (DMD). Skeletal muscle fibres, as well as cultured skeletal muscle cells from *mdx* mice, have been and are still widely used to attempt to understand how the absence of dystrophin in DMD patients leads to the devastating muscle degeneration process that they undergo. Since the late eighties, it has been repeatedly suggested that, in dystrophin-deficient muscle cells, an elevated intracellular free calcium concentration ($[Ca^{2+}]_i$), due to a deficient regulation of cytosolic $[Ca^{2+}]$ at the sarcolemmal level, may be responsible for muscle necrosis (Turner *et al.* 1988; Fong *et al.* 1990; Turner *et al.* 1991; Bakker *et al.* 1993; Denetclaw *et al.* 1994; Hopf *et al.* 1996; Tutdibi *et al.* 1999). This hypothesis has, however, been seriously challenged, as several other lines of study failed to detect elevated $[Ca^{2+}]_i$ levels in dystrophic preparations under similar experimental conditions (Gailly *et al.* 1993; Head, 1993; Pressmar *et al.* 1994; Leijendekker *et al.* 1996). Although attempts have been made to interpret the differences between results on the basis of specific details of experimental procedures and/or of preparation of cells (see for instance Hopf *et al.* 1996), the question has still not been convincingly settled (see for review Gillis, 1996). Analysis of $[Ca^{2+}]_i$ transients induced by membrane depolarization should have helped to resolve this question, as such data have for a long time proved to be efficient in gaining insights into the properties of the various systems involved in $[Ca^{2+}]_i$ regulation (see for instance Melzer *et al.* 1995). However, within the available data, a controversy also stands regarding the properties of the $[Ca^{2+}]_i$ transients in control and *mdx* muscle cells: in particular, results from Turner *et al.* (1988, 1991) and Tutdibi *et al.* (1999), in conditions of field stimulation, suggested that calcium transients displayed a slower time course of decay in *mdx* than in control fibres, whereas Head (1993) reported no difference in fibres stimulated through a single intracellular microelectrode. Considering the fundamental importance of these issues for understanding the DMD pathology, there is interest in

bringing new data into the debate. Within the present study, using indo-1 as calcium indicator, we measured resting $[Ca^{2+}]_i$ in skeletal muscle fibres isolated from control and *mdx* mice. Furthermore, taking advantage of a recently developed voltage-clamp technique (Jacquemond, 1997), we also measured changes in $[Ca^{2+}]_i$ elicited by controlled membrane depolarizations. Finally, since in the *mdx* mouse it is known that intense muscle degeneration only occurs during a transient period that starts at about 2 weeks of age (Carnwath & Shotton, 1987; DiMario *et al.* 1991) and is, for unclear reasons, followed by a persistent stable situation that allows the animal to enjoy normal muscular function, we attempted to compare data from fibres isolated from control and *mdx* mice of various ages. Preliminary aspects of this work have been presented in abstract form (Collet *et al.* 1999).

METHODS

Preparation of the muscle fibres

Experiments were performed on single skeletal fibres isolated from the flexor digitorum brevis and interosseus muscles of wild-type (C57BL/10ScSn) and *mdx* (C57BL/10*mdx*) male mice aged ~2–50 weeks. All experiments were performed in accordance with the guidelines of the French Ministry of Agriculture (87/848) and of the European Community (86/609/EEC). Details of procedures for enzymatic isolation of single fibres, partial insulation of fibres with silicone grease and intracellular dye loading were as described previously (Jacquemond, 1997). In brief, mice were killed by cervical dislocation following halothane anaesthesia. The muscles were removed and treated with collagenase (Sigma, Type 1) for 60–75 min at 37 °C in the presence of Tyrode solution as the external solution. Single fibres were then obtained by triturating the muscles within the experimental chamber. The length of the fibres typically ranged between 300 and 600 μm. Control and *mdx* fibres that were used in the present study had mean diameters of $45{\cdot}3 \pm 1$ μm ($n = 74$) and $44{\cdot}1 \pm 2$ μm ($n = 64$), respectively. When considering only the control and *mdx* fibres from which calcium transients were measured in response to membrane depolarizations, the mean diameters were 51 ± 2 μm ($n = 33$) and 48 ± 3 μm ($n = 34$), respectively. The major part of a single fibre was electrically insulated with silicone grease so that whole-cell voltage clamp could be achieved on a short portion (50–100 μm long) of the fibre extremity (Jacquemond, 1997). The mean lengths of the silicone-free portion of control and *mdx* fibres used in this study were $87{\cdot}2 \pm 3$ μm ($n = 74$) and $96{\cdot}5 \pm 4$ μm ($n = 64$), respectively. When considering only the control and *mdx* fibres from which calcium transients were measured in response to membrane depolarizations, the mean lengths of the silicone-free portion of the fibres were 81 ± 4 μm ($n = 33$) and 91 ± 4 μm ($n = 34$), respectively. Intracellular indo-1 loading was then performed through local pressure microinjection with a micropipette containing 0·5 mM indo-1 (pentapotassium salt, Molecular Probes Inc.) dissolved in a 140 mM potassium aspartate-containing solution (or a 140 mM potassium glutamate-containing solution). Indo-1 microinjection was carried out with the pipette tip inserted through the silicone within the insulated part of the fibre.

All experiments were performed at room temperature (20–22 °C), in the presence of the standard tetraethylammonium (TEA)-containing solution as the extracellular medium (see 'Solutions').

Electrophysiology

An RK-400 patch-clamp amplifier (Bio-Logic, Claix, France) was used in the whole-cell configuration. Command voltage pulse generation and data acquisition were done using commercial software (Biopatch Acquire, Bio-Logic) driving an A/D, D/A converter (Lab Master DMA board, Scientific Solutions Inc., Solon, OH, USA). Analog compensation was systematically used to decrease the effective series resistance. Voltage clamp was usually performed with a microelectrode filled with a solution containing 3 M potassium acetate and 20 mM KCl (Jacquemond, 1997). However, in one series of experiments, we used microelectrodes filled with an internal-like solution containing (mM): 120 potassium glutamate, 5 Na_2-ATP, 5 Na_2-phosphocreatine, 5·5 $MgCl_2$, 5 glucose and 5 Hepes, adjusted to pH 7·2 with KOH. In this case, the microelectrodes had blunt tips so that their resistance was in the same range as the potassium acetate-containing microelectrodes (1·5–4 MΩ). This procedure was recently adopted because it was found to improve the stability of the measurements over long periods of time. Data that were obtained under these conditions correspond to measurements taken from the batch of control and *mdx* fibres obtained from mice older than 35 weeks. They are presented in the last section of Results.

In all cases, the tip of the microelectrode was inserted through the silicone, within the insulated part of the fibre. Membrane depolarizations were always applied from a holding command potential of −80 mV. The mean capacitance measured from the fibres used for the calcium measurements described in this paper was 628 ± 36 pF ($n = 38$) for control fibres and 700 ± 47 pF ($n = 34$) for *mdx* fibres. The mean input resistance calculated from the steady change in membrane current elicited by a 20 mV hyperpolarizing command step of 20 ms duration was $17{\cdot}4 \pm 2$ MΩ ($n = 38$) for control fibres and 19 ± 2 MΩ ($n = 34$) for *mdx* fibres.

In a few fibres, the change in membrane potential elicited by command voltage steps was followed by an additional microelectrode filled with 3 M KCl, using a high-input impedance voltage amplifier (VF 1800, Bio-Logic). Figure 1 shows an example of such records (noisy traces) recorded in response to 20 ms command steps (superimposed continuous lines) of 20, −20 and −40 mV applied to the preparation with the patch-clamp amplifier. The inset shows the same records after scaling by the corresponding change in command voltage. In five fibres where such measurements were performed, the amplitude of the measured change in membrane potential was 90–95% of the amplitude of the command pulse.

Fluorescence measurements

The optical set-up for indo-1 fluorescence measurements was described previously (Jacquemond, 1997). In brief, a Nikon Diaphot epifluorescence microscope was used in diafluorescence mode. For indo-1 excitation, the beam of light from a high-pressure mercury bulb set on the top of the microscope was passed through a 335 nm interference filter and focused onto the preparation using a quartz aspherical doublet. The emitted fluorescence was collected by a ×40 objective and simultaneously detected at 405 nm (F_{405}) and 470 nm (F_{470}) by two photomultipliers. The fluorescence measurement field was 40 μm in diameter and the silicone-free extremity of each tested fibre was placed in the middle of the field. Fluorescence signals were digitized and stored on disk using the same hardware and software as for the electrophysiological measurements. Background fluorescence at both emission wavelengths was measured next to each tested fibre and was then subtracted from all measurements. On each fibre, a fluorescence measurement was taken before impaling the fibre with the microelectrode used for voltage clamp. These data were used to

determine what is referred to as the initial resting free calcium concentration.

Calibration of the indo-1 response and $[Ca^{2+}]_i$ calculation

Free calcium concentration ($[Ca^{2+}]$) was calculated using the standard ratio method (Grynkiewicz *et al.* 1985), with the parameters: $R = F_{405}/F_{470}$, and R_{min}, R_{max}, K_D and β having their usual definitions. No correction was made for indo-1 Ca^{2+} binding and dissociation kinetics, so that the derived time course of change in $[Ca^{2+}]$ does not reflect the true time course of change in ionised free calcium concentration. Results were either expressed in terms of indo-1 percentage saturation or in actual free calcium concentration (for details of calculation, see Jacquemond, 1997; Csernoch *et al.* 1998). The value of K_D was assumed to be identical in control and *mdx* fibres and equal to 300 nM. *In vivo* values for R_{min}, R_{max} and β were measured in control and in *mdx* fibres using procedures described previously (Jacquemond, 1997). For the determination of R_{min} and R_{max}, fibres were completely embedded in silicone grease, pressure microinjected with indo-1, and then after dye equilibration, microinjected with a solution containing either 0·5 M EGTA or 1 M $CaCl_2$, respectively. The 0·5 M EGTA solution was adjusted to pH 7·20 with KOH. The value of β was determined from the slope of plots of F_{470} traces *versus* F_{405} traces recorded simultaneously in response to membrane depolarizations (see Jacquemond, 1997). The values of R_{min}, R_{max} and β were measured in control and *mdx* fibres from mice of various ages. In control, R_{min}, R_{max} and β were obtained in fibres from mice aged ~5–50, 6–50 and 3–50 weeks. In *mdx*, R_{min}, R_{max} and β were obtained in fibres from mice aged ~9–40, 4–40 and 4–41 weeks. No age dependence of any of these parameters could be detected in control and *mdx* fibres (not shown). None of the calibration parameter values was significantly different between control and *mdx* fibres. In control fibres, mean values for R_{min} and R_{max} were $0{\cdot}55 \pm 0{\cdot}02$ ($n = 27$) and $3{\cdot}4 \pm 0{\cdot}2$ ($n = 26$), respectively; in *mdx* fibres, they were $0{\cdot}58 \pm 0{\cdot}03$ ($n = 17$) and $3{\cdot}0 \pm 0{\cdot}2$ ($n = 34$), respectively. The mean value of β was $2{\cdot}13 \pm 0{\cdot}03$ ($n = 36$) in control fibres and $2{\cdot}16 \pm 0{\cdot}03$ ($n = 33$) in *mdx* fibres.

Within the present study, 14 out of 86 control fibres and 11 out of 68 *mdx* fibres displayed an initial resting R value that was lower than the mean R_{min} value measured from the fibres injected with EGTA. Although meaningless, the mean R values from these fibres would have corresponded to indo-1 saturation levels of '−6%' and '−8%' in control and *mdx* fibres, respectively. Fibres displaying such low R values were found in batches of fibres from mice ranging between 3 and 18 weeks of age in control, and 4 and 41 weeks of age in *mdx*. The reason for fibres displaying such low R values is unclear. It may be due to specific alteration of the spectral properties of indo-1 in these fibres from an unknown origin. Alternatively, it may also be related to difficulties in accurately assessing the value of R_{min} within the intracellular environment. One possibility could be that R_{min} was underestimated due to a reduced affinity of EGTA for Ca^{2+} that could occur as a consequence of a drop in pH following release of H^+ from EGTA upon binding of endogenous Ca^{2+}. This possibility was experimentally tested by comparing the values of R_{min} measured either by using the regular EGTA-containing solution, or by including a pH buffer in the EGTA-containing solution. Fibres from an *mdx* mouse were injected either with the standard 0·5 M EGTA solution or with the same solution to which 0·2 M Pipes was added. The pH of the Pipes-containing solution was also adjusted to 7·20 with KOH. In seven fibres injected with the 0·5 M EGTA solution, the mean ± S.E.M. R_{min} value was $0{\cdot}58 \pm 0{\cdot}04$, whereas in seven fibres injected with 0·5 M EGTA plus 0·2 M Pipes, the mean R_{min} value was $0{\cdot}53 \pm 0{\cdot}02$. These values are not significantly different ($P = 0{\cdot}2$) and we thus believe that the possibility that an intracellular pH change may have led to an underestimation of R_{min} is quite unlikely. However, other problems may lead to difficulties in R_{min} determination, as, for instance, high intracellular EGTA concentrations were previously found to have unexpected effects on the fluorescence ratio of fura-2 in frog skeletal muscle fibres (Klein *et al.* 1988). In our case, rather than arbitrarily setting the R_{min} value to a level compatible with all data, fibres showing resting R values lower than R_{min} were excluded from the analysis.

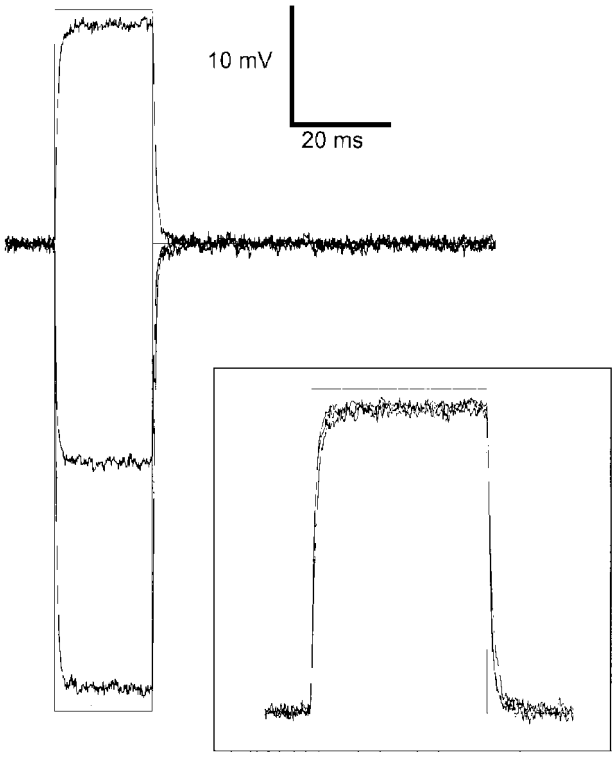

Figure 1. Changes in membrane potential recorded in response to voltage-clamp depolarizations

The noisy traces correspond to the changes in membrane potential, recorded with a single microelectrode, in response to 20 ms voltage-clamp command steps (superimposed continuous lines) of 20, −20 and −40 mV applied to the skeletal muscle fibre with the patch-clamp amplifier. The inset shows the same records after scaling by the corresponding change in command voltage.

Solutions

Tyrode solution contained (mM): 140 NaCl, 5 KCl, 2·5 $CaCl_2$, 1 $MgCl_2$ and 10 Hepes, adjusted to pH 7·4 with NaOH. Standard external solution contained (mM): 140 TEA-methanesulfonate, 2·5 $CaCl_2$, 2 $MgCl_2$, 10 TEA-Hepes and 0·002 tetrodotoxin, pH 7·2.

Statistics

Least-squares fits were performed using a Marquardt-Levenberg algorithm routine included in Microcal Origin (Microcal software Inc., Northampton, MA, USA). Data values are presented as means ± S.E.M. Statistical significance was determined using a two-tailed t test assuming significance for $P < 0{\cdot}05$.

RESULTS

Initial resting $[Ca^{2+}]_i$

The top panels of Fig. 2 show the individual values of initial resting $[Ca^{2+}]_i$ measured in control (left) and *mdx* fibres (right). $[Ca^{2+}]_i$ values were plotted *versus* the age of the mice from which muscle fibres were isolated. The bottom panels show values of resting $[Ca^{2+}]_i$ from mice of similar ages averaged over a period arbitrarily set to every consecutive 10 weeks. Although there was a wide scattering of the data, most of the control and *mdx* fibres displayed an initial resting $[Ca^{2+}]_i$ ranging between ~10 and 100 nM. Mean values from all control and *mdx* fibres were 56 ± 5 nM ($n = 72$) and 48 ± 7 nM ($n = 57$), respectively, indicating no significant difference between the two groups ($P > 0{\cdot}3$). However, in a batch of fibres from *mdx* mice ~40 weeks old, the initial resting $[Ca^{2+}]_i$ was surprisingly low compared, for instance, to fibres from control mice aged ~50 weeks. Fibres from mice younger than 35 weeks displayed a mean initial resting $[Ca^{2+}]_i$ of 52 ± 4 nM in control ($n = 58$) *versus* 55 ± 1 nM in *mdx* ($n = 46$), respectively. In fibres from mice older than 35 weeks, the mean initial resting $[Ca^{2+}]_i$ was 16 ± 4 nM in *mdx* ($n = 11$), which was significantly lower than that in 14 control fibres (71 ± 10 nM, $P < 0{\cdot}0002$). In case the difference may somehow reflect an age dependence of the regulation of $[Ca^{2+}]_i$ in *mdx* fibres, in the subsequent part of this work calcium transients were compared in control and *mdx* fibres from mice younger and older than 35 weeks.

As specified in the Methods section, 16% of all control and *mdx* fibres exhibited indo-1 fluorescence ratio values that were less than the R_{min} value, and they were not included in the results. Although this introduces some doubt as to the accuracy of our $[Ca^{2+}]_i$ determination, it should be mentioned that including these fibres in the resting measurements, but comparing control and *mdx* fibres in terms of fluorescence ratio values rather than $[Ca^{2+}]_i$ values, would lead to the same conclusions regarding resting levels in control and *mdx* fibres (not shown).

Finally, it should be noted that not all fibres from which an initial resting $[Ca^{2+}]_i$ measurement was taken were then challenged by depolarizing pulses, so that the number of fibres in the following sections is less than the total number presented in Fig. 2.

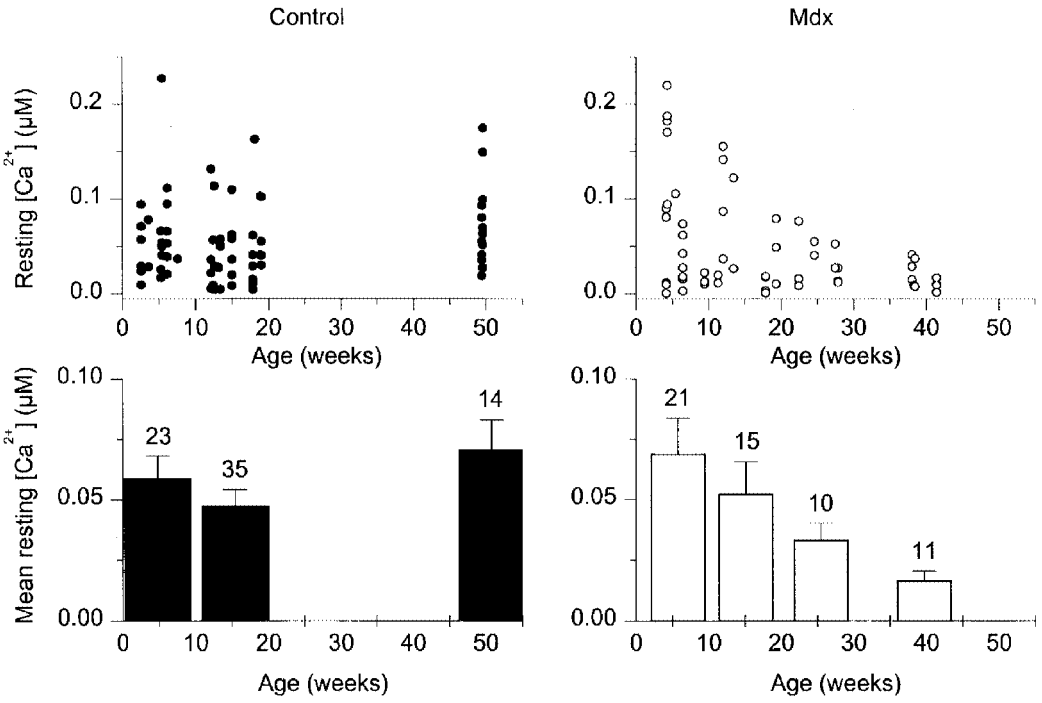

Figure 2. Initial resting $[Ca^{2+}]_i$ in control and *mdx* muscle fibres

The top panels show the individual values of initial resting $[Ca^{2+}]_i$ measured in 72 control (left) and 57 *mdx* fibres (right). $[Ca^{2+}]_i$ values are plotted *versus* the age of the mice from which muscle fibres were isolated. The bottom panels show the corresponding mean and S.E.M. values of resting $[Ca^{2+}]_i$ from mice of similar ages; these values were obtained from averaging data points over a period arbitrarily set to every consecutive 10 weeks. The number of fibres is indicated above each corresponding bar.

Calcium transients in response to depolarizing pulses in a batch of control and *mdx* fibres displaying a similar initial resting $[Ca^{2+}]_i$

In this section, we compare calcium transients recorded from a batch of control and *mdx* fibres isolated from mice younger than 35 weeks (3–18 weeks and 4–28 weeks old, respectively). As specified in the previous section, within this age bracket, the mean initial resting $[Ca^{2+}]_i$ was similar in the two groups. Data that are presented were obtained from fibres which, after setting the holding command potential at −80 mV, were first depolarized either by a series of short pulses to 0 mV of increasing duration, or by 50 ms duration command pulses to −50, −40, −30, −20, −10 and 0 mV.

Figure 3*A* shows a representative series of indo-1 percentage saturation traces from a control (left) and an *mdx* fibre (right) in response to 5, 15 and 25 ms duration command pulses to 0 mV (V_c, bottom traces). Qualitatively, the general pattern and maximal amplitude of the respective changes in indo-1 saturation were similar in the two fibres. The 5 ms duration pulse induced a transient rise in indo-1 saturation from a resting level close to 10% up to a maximum of ~60%. Increasing the duration of the pulse to 15 and 25 ms produced an increase in the peak saturation up to ~80% together with a more delayed return of the signal down towards the resting level. At the end of each record, the indo-1 saturation level was higher than the initial resting level before the pulse. However, within the interpulse period (set to 30 s), the signal returned to its initial value. Figure 3*B* shows the $[Ca^{2+}]_i$ transients calculated from the corresponding indo-1 percentage saturation traces of Fig. 3*A*. In the control and in the *mdx* fibre, $[Ca^{2+}]_i$ rose up to a maximum of ~0·4 μM in response to the 5 ms pulse and to ~1 μM in response to the 15 and 25 ms pulses. A single exponential plus constant function was fitted to the

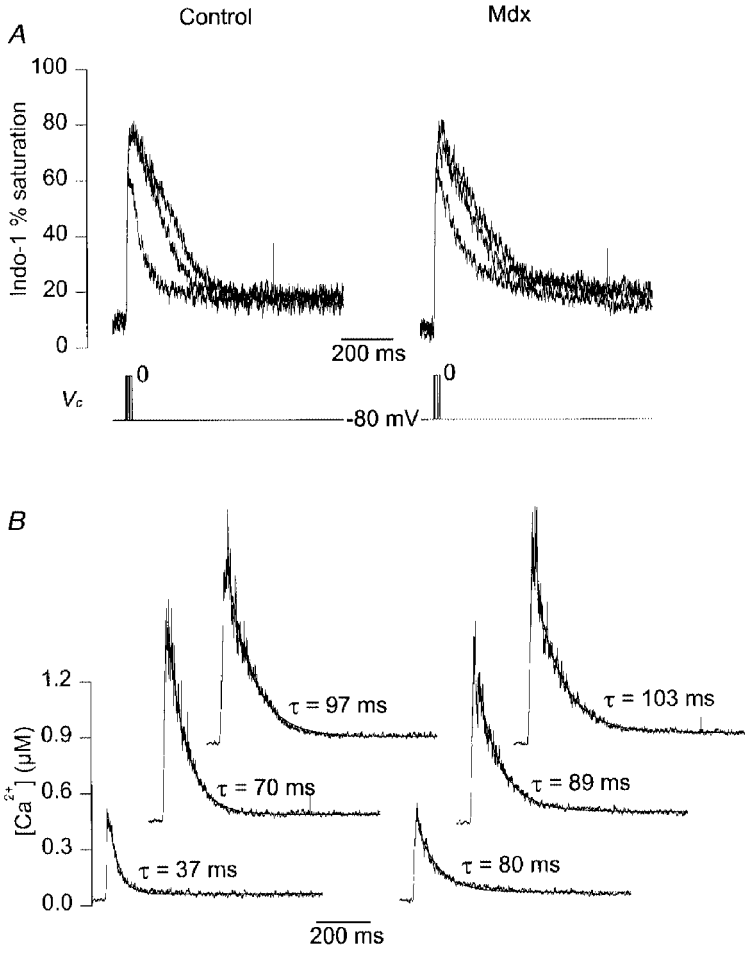

Figure 3. Indo-1 calcium transients elicited by short depolarizing pulses in a control and in an *mdx* fibre exhibiting a similar resting $[Ca^{2+}]_i$

A, indo-1 percentage saturation traces from a control (left) and an *mdx* fibre (right) in response to 5, 15 and 25 ms duration command pulses to 0 mV (V_c, bottom traces). The control and the *mdx* fibre were from a 13- and a 7-week-old mouse, respectively. *B*, $[Ca^{2+}]_i$ transients calculated from the above corresponding indo-1 percentage saturation traces. For clarity, $[Ca^{2+}]_i$ traces elicited by pulses of increasing duration are shifted in the *x* and *y* direction. The smooth curves superimposed on the decay of the $[Ca^{2+}]_i$ traces correspond to the results from fitting a single exponential plus constant function. The value of the corresponding time constant is indicated next to each trace.

decay phase of the $[Ca^{2+}]_i$ transients starting 20 ms after the end of the pulses. It must be mentioned that such exponential fits were only performed when the peak $[Ca^{2+}]_i$ did not exceed ~2 μM. For higher peak $[Ca^{2+}]_i$, the combination of heavy indo-1 saturation together with the noise in the records usually made the estimation of the time constant quite unreliable. The fits are shown as smooth curves superimposed on the $[Ca^{2+}]_i$ traces, and the value of the time constant of decay (τ) is indicated next to each corresponding trace. Following the 5 ms duration depolarizing step, the $[Ca^{2+}]_i$ decay was about 2 times slower ($\tau = 80$ ms) in the *mdx* fibre than in the control fibre ($\tau = 37$ ms). Following the more prolonged depolarizations, the $[Ca^{2+}]_i$ decay proceeded at a much closer rate in the control and *mdx* fibre: after the 15 and 25 ms duration pulses, values for the time constant of $[Ca^{2+}]_i$ decay in the *mdx* fibre were ~1·3 and 1·1 times that of the control fibre, respectively.

Figure 4 shows the mean (continuous trace) ± S.E.M. (vertical lines) indo-1 percentage saturation traces elicited by 5 and 15 ms depolarizing pulses at 0 mV in 10 control (left) and 7 *mdx* fibres (right). Of all fibres on which such short pulses were first applied after voltage clamping at −80 mV, four *mdx* fibres and one control fibre exhibited an initial indo-1 saturation level higher than 20%. They were included neither in the mean traces shown in Fig. 4*A*, nor in the results of the analysis shown in Fig. 4*B*, in order to maintain the goal for this set of measurements of comparing signals from control and *mdx* fibres displaying a similar resting $[Ca^{2+}]_i$. Including these fibres did not change the

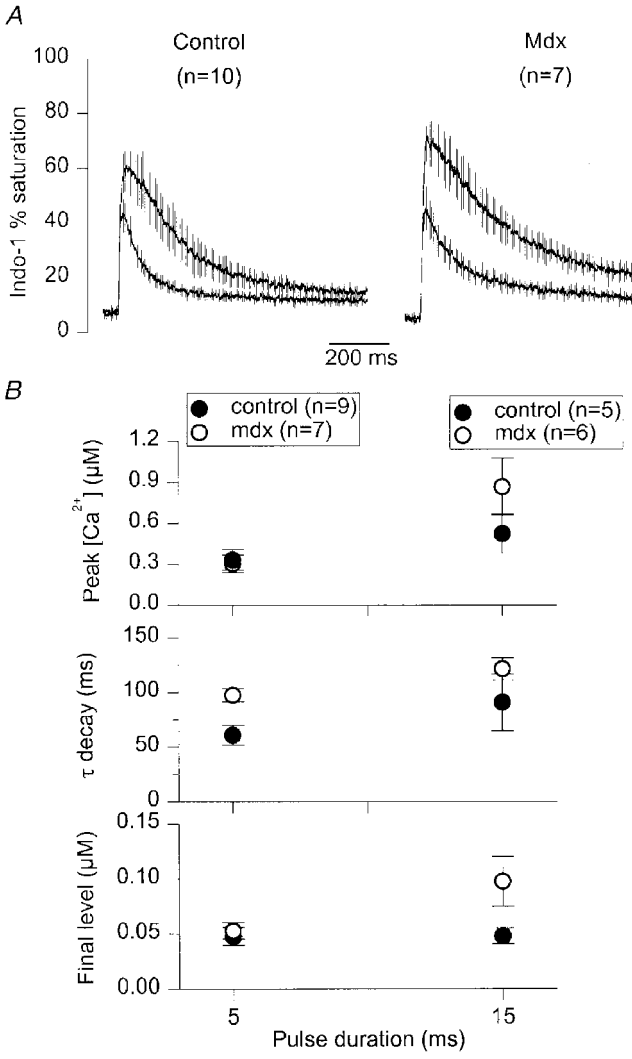

Figure 4. Average properties of indo-1 calcium transients elicited by short depolarizing pulses in a batch of control and *mdx* muscle fibres exhibiting similar resting $[Ca^{2+}]_i$ levels

A, mean (continuous trace) ± S.E.M. (vertical lines) indo-1 percentage saturation traces elicited by 5 and 15 ms depolarizing pulses at 0 mV in 10 control (left) and 7 *mdx* fibres (right). *B*, from top to bottom, mean ± S.E.M. values of peak $[Ca^{2+}]_i$, time constant of $[Ca^{2+}]_i$ decay and final $[Ca^{2+}]_i$ level measured from the individual control and *mdx* $[Ca^{2+}]_i$ traces on which exponential fits were performed. The number of fibres used for each pulse duration is indicated at the top of *B*.

results of the analysis (not shown). However, as a high resting $[Ca^{2+}]_i$ may have been suspected to influence the saturation of intrinsic Ca^{2+} buffers, and thus the Ca^{2+} removal capability of the fibres, it seemed more reasonable to restrict the comparison to fibres that displayed similar levels of initial resting $[Ca^{2+}]_i$. The mean ± S.E.M. time constant of decay and final $[Ca^{2+}]_i$ level estimated from fitting a single exponential plus constant function to the decay phase of the $[Ca^{2+}]_i$ signals are presented in Fig. 4*B* (middle and lower plot, respectively); the upper plot shows the mean peak $[Ca^{2+}]_i$ from the traces on which exponential fits were performed.

In response to a 5 ms duration pulse, the mean peak $[Ca^{2+}]_i$ was 0·33 ± 0·07 and 0·3 ± 0·06 μM in nine control and six *mdx* fibres, respectively, and thus not significantly different ($P > 0·7$). For the same fibres, the mean value of the $[Ca^{2+}]_i$ decay time constant was significantly larger in the *mdx* than in the control fibres (97 ± 6 ms compared to 61 ± 9 ms, $P = 0·01$), while the final steady levels were similar (48 ± 8 nM in control *versus* 53 ± 7 nM in *mdx*, $P > 0·6$). In response to a 15 ms duration pulse, mean values of peak $[Ca^{2+}]_i$, time constant of $[Ca^{2+}]_i$ decay, and final $[Ca^{2+}]_i$ level were not significantly different in control and *mdx* fibres.

The voltage dependence of the change in $[Ca^{2+}]_i$ was examined by applying successive 50 ms depolarizing pulses of increasing amplitude. Figure 5*A* shows indo-1 percentage saturation traces obtained in response to depolarizing command steps of 50 ms duration at −40, −30, −20, −10, 0

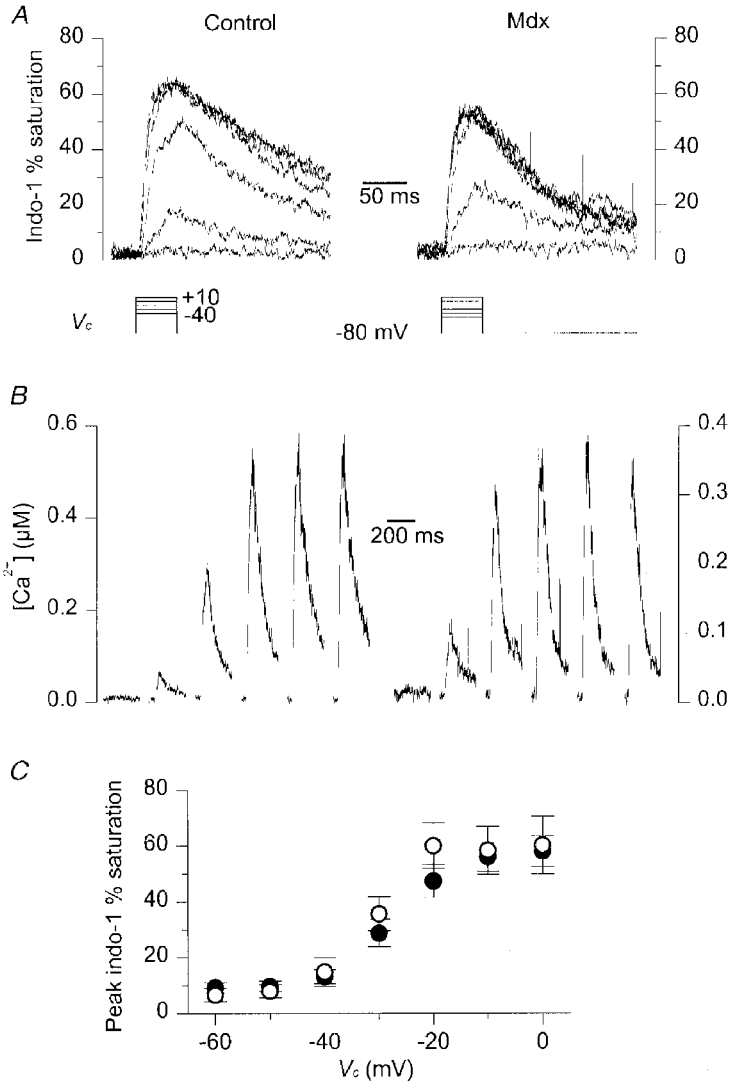

Figure 5. Indo-1 calcium transients elicited by 50 ms depolarizing pulses of increasing amplitude in a control and in an *mdx* fibre exhibiting a similar resting $[Ca^{2+}]_i$

A, indo-1 percentage saturation traces from a control (left) and an *mdx* fibre (right) in response to depolarizing command steps at −40, −30, −20, −10, 0 and +10 mV (V_c, bottom traces). The control and the *mdx* fibre were from a 13- and an 11-week-old mouse, respectively. *B*, $[Ca^{2+}]_i$ transients calculated from the above corresponding indo-1 percentage saturation traces; traces are displayed for pulses of increasing amplitude from left to right. *C*, mean ± S.E.M. indo-1 peak percentage saturation measured in response to 50 ms depolarizations at various command potentials. ●, control fibres ($n = 14$); ○, *mdx* fibres ($n = 6$).

and +10 mV in a control (left) and in an *mdx* fibre (right). In Fig. 5*B*, the corresponding $[Ca^{2+}]_i$ traces are shown for pulses of increasing amplitude from left to right. In both fibres, the threshold for detecting a clear increase in $[Ca^{2+}]_i$ was at −30 mV. For more depolarized values, the peak indo-1 percentage saturation and corresponding $[Ca^{2+}]_i$ were increased and reached a quasi-constant level for potentials more positive than −10 mV. For a given value of step depolarization, the peak $[Ca^{2+}]_i$ was more elevated in the control fibre than in the *mdx* one. However, this was not a common feature of these responses; the dependence of the mean maximal amplitude of the indo-1 saturation upon the command membrane potential is presented in Fig. 5*C*. For command potentials that did not elicit any change in indo-1 saturation (below the threshold), the values of peak saturation actually correspond to the mean of the overall saturation traces. Mean results were presented in terms of indo-1 saturation rather than as actual $[Ca^{2+}]_i$ because some fibres displayed peak values corresponding to very high levels of indo-1 saturation, for which the $[Ca^{2+}]_i$ was poorly determined. Nevertheless, the results seem to indicate that, within the limits of the method, there was no detectable significant difference between control and *mdx* fibres in terms of the voltage dependence of peak $[Ca^{2+}]_i$.

Calcium transients in response to depolarizing pulses in a batch of *mdx* fibres displaying a lower initial resting $[Ca^{2+}]_i$ than control fibres

As described in relation to Fig. 2, fibres isolated from the oldest *mdx* mice that were used in the present study (~40 weeks old) exhibited a substantially lower resting $[Ca^{2+}]_i$ than control fibres from either younger or older mice.

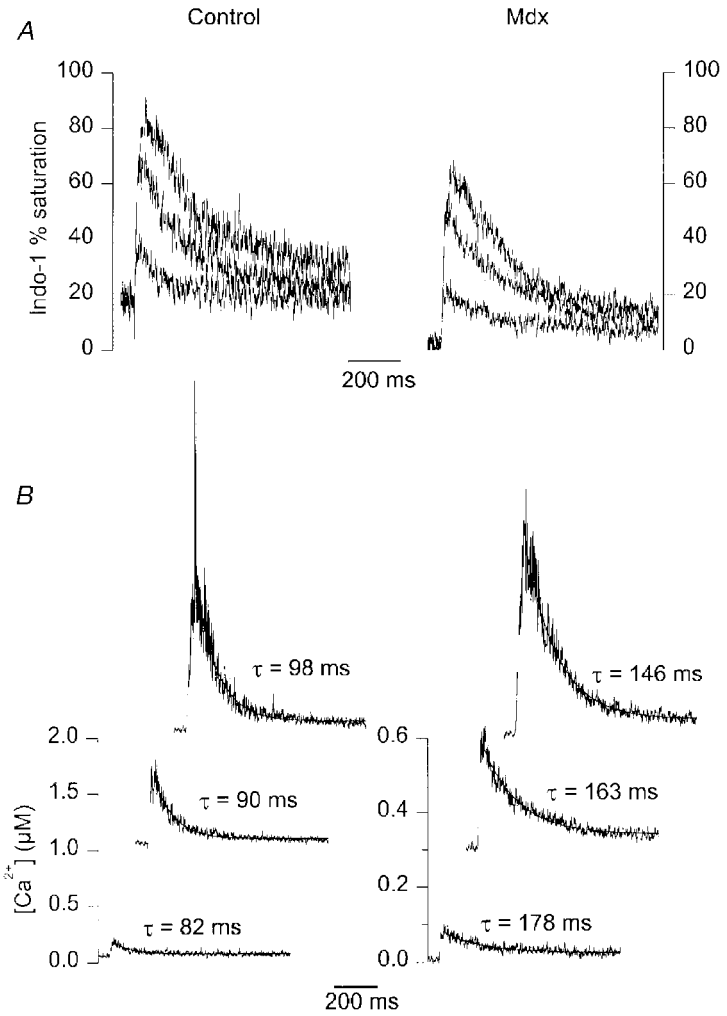

Figure 6. Indo-1 calcium transients elicited by depolarizing pulses at 0 mV of increasing duration in a control and in an *mdx* fibre from a batch of mice older than ~35 weeks

The *mdx* fibres from this batch displayed a significantly lower mean resting $[Ca^{2+}]_i$ than control ones. *A*, a series of indo-1 percentage saturation traces from a control (left) and an *mdx* fibre (right) in response to 5, 15 and 45 ms duration command pulses at 0 mV. The control and *mdx* fibre were from a 50- and a 41-week-old mouse, respectively. *B*, $[Ca^{2+}]_i$ transients calculated from the above corresponding indo-1 percentage saturation traces. The smooth curves superimposed on the decay of the $[Ca^{2+}]_i$ traces correspond to the results from fitting a single exponential plus constant function. The value of the corresponding time constant is indicated next to each trace.

In this section, depolarization-induced calcium transients in fibres from this batch were compared to those from fibres isolated from control mice aged ~50 weeks.

Figures 6 and 7 are presented in the same format as Figs 3 and 4, respectively. All data correspond to the first responses that were elicited from each fibre after voltage clamping. Figure 6*A* shows a series of indo-1 percentage saturation traces from a control (left) and an *mdx* fibre (right) in response to 5, 15 and 45 ms duration command pulses to 0 mV. As compared to results shown in Fig. 3, one main difference was the lower level of resting indo-1 saturation in the *mdx* fibre (~3%) than in the control one (~15%). In the control fibre, the 5 ms duration pulse induced a transient rise in indo-1 saturation up to a maximum of ~40%. In the *mdx* fibre, an identical pulse induced a transient rise up to ~20%. As previously observed for the traces shown in Fig. 3, increasing the duration of the pulse produced an increase in the peak saturation and a more delayed return of the signal to the resting level. However, peak saturation always remained lower in the *mdx* fibre than in the control one. Figure 6*B* shows the $[Ca^{2+}]_i$ transients calculated from the corresponding indo-1 percentage saturation traces of Fig. 6*A*. Again, the result of fitting a single exponential plus constant function to the $[Ca^{2+}]_i$ decay is shown as a smooth curve superimposed on the corresponding $[Ca^{2+}]_i$ trace, with the value of the time constant indicated next to each trace. In this example, the time constant was larger in the *mdx* than in the control fibre for all three $[Ca^{2+}]_i$ transients. The difference was more marked for the shortest pulse: the ratio

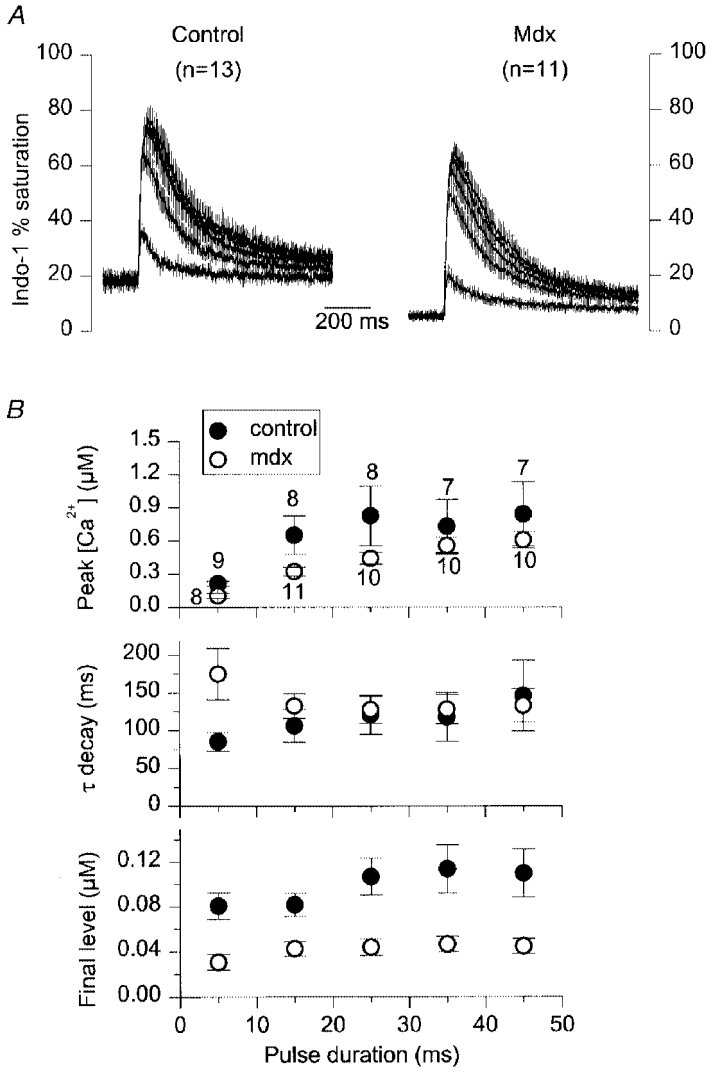

Figure 7. Average properties of indo-1 calcium transients elicited by depolarizing pulses of increasing duration in fibres from a batch of control and *mdx* mice older than ~35 weeks

A, mean (continuous trace) ± S.E.M. (vertical lines) indo-1 percentage saturation traces elicited by 5, 15, 25, 35 and 45 ms depolarizing pulses at 0 mV in 13 control (left) and 11 *mdx* fibres (right). *B*, from top to bottom, mean ± S.E.M. values of peak $[Ca^{2+}]_i$, time constant of $[Ca^{2+}]_i$ decay and final $[Ca^{2+}]_i$ level, measured from the individual control and *mdx* $[Ca^{2+}]_i$ traces on which exponential fits were performed. The number of fibres used for each pulse duration is indicated next to the peak $[Ca^{2+}]_i$ data points in *B*.

of the time constant of decay in the *mdx* fibre to the one in the control fibre was 2·2, 1·8 and 1·5 for the 5, 15 and 45 ms pulses, respectively.

Figure 7*A* shows a family of mean (continuous trace) ± S.E.M. (vertical lines) indo-1 percentage saturation traces in response to step command depolarizations at 0 mV of increasing duration (5–45 ms with a 10 ms increment). Again, apart from a lower level of resting and peak saturation in the mean *mdx* traces, no clear difference in the overall time course of the transients was apparent between control and *mdx*. The mean ± S.E.M. time constant of decay and final $[Ca^{2+}]_i$ level estimated from fitting a single exponential plus constant function to the decay phase of the individual $[Ca^{2+}]_i$ signals are presented in Fig. 7*B* (middle and lower plot, respectively); the upper plot shows the mean peak $[Ca^{2+}]_i$ from the traces on which exponential fits were performed.For each pulse duration, the mean peak $[Ca^{2+}]_i$ was larger in the control than in the *mdx* fibres; this was, however, only significant for the 5 and 15 ms duration pulses, with P values of 0·001 and 0·04, respectively. For pulses longer than 5 ms the mean time constant of $[Ca^{2+}]_i$ decay was not significantly different between control and *mdx* fibres. Only for the 5 ms duration pulse was the mean $[Ca^{2+}]_i$ decay time constant significantly larger in *mdx* (175 ± 34 ms, $n = 8$) than in control fibres (85 ± 12 ms, $n = 9$), with $P = 0{\cdot}02$. Interestingly, in the *mdx* fibres, this resulted in a larger mean time constant for the 5 ms pulse than for the 15 ms one, whereas the opposite relationship was observed in control fibres, and in *mdx* fibres from mice younger than 35 weeks. Regarding the final $[Ca^{2+}]_i$ level, it was always significantly lower in *mdx* than in control fibres, which is in agreement with the lower resting $[Ca^{2+}]_i$ in *mdx* fibres before the pulses.

In most control and *mdx* fibres from this same batch, a series of 50 ms duration pulses of increasing amplitude was applied after the pulses at 0 mV of increasing duration, the results from which were described above. Figure 8*A* shows a series of indo-1 percentage saturation traces obtained in response to 50 ms duration depolarizations to −40, −30, −20, −10, 0 and +10 mV in a control (left) and in an *mdx* fibre (right). Resting saturation was higher in the control than in the *mdx* fibre. In the control fibre, for a given pulse amplitude, the peak saturation was also larger than in the *mdx* fibre: for instance, in response to the pulse to +10 mV, peak indo-1 percentage saturation reached ∼90% in the control compared to ∼65% in the *mdx* fibre. Figure 8*B* shows the dependence of the mean peak indo-1 percentage saturation upon the command potential from this series of measurements. For all values of command potential, mean values were larger in the control than in the *mdx* fibres. This was, however, only very significant for subthreshold values (−60 to −40 mV, $P < 0{\cdot}003$) corresponding to resting

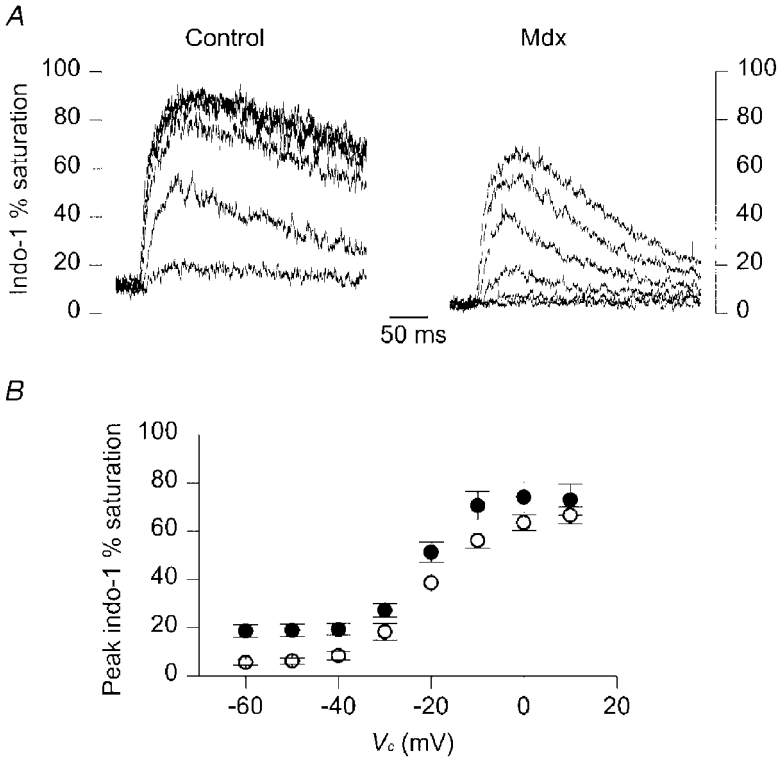

Figure 8. Indo-1 calcium transients elicited by 50 ms depolarizing pulses of increasing amplitude in control and in *mdx* fibres from a batch of mice older than ∼35 weeks

A, indo-1 percentage saturation traces from a control (left) and an *mdx* fibre (right) in response to depolarizing command steps at −40, −30, −20, −10, 0 and +10 mV. The control and *mdx* fibre were from a 50- and a 38-week-old mouse, respectively. *B*, mean ± S.E.M. indo-1 peak percentage saturation measured in response to 50 ms depolarizations at various command potentials (V_c). ●, control fibres ($n = 11$); ○, *mdx* fibres ($n = 11$).

$[Ca^{2+}]_i$ levels. For depolarizations at −20 and −10 mV, values were significantly different ($P = 0{\cdot}03$ and 0·04, respectively). Values were not significantly different for depolarizations at −30 mV ($P = 0{\cdot}06$) or for those at 0 and +10 mV ($P > 0{\cdot}1$). Again, data were not expressed in terms of mean $[Ca^{2+}]_i$ levels because, particularly in control fibres, the peaks of the transients were too close to full indo-1 saturation to give reliable estimates of $[Ca^{2+}]_i$. For instance, for the pulses at +10 mV, the difference in mean peak saturation between control and *mdx* fibres was less than 10 %, but the corresponding mean peak $[Ca^{2+}]_i$, calculated from the individual values of peak saturation, was more than 4 times larger in control than in *mdx* fibres (not shown).

DISCUSSION

Resting $[Ca^{2+}]_i$

Under our experimental conditions, the resting $[Ca^{2+}]_i$ was not found to be chronically elevated in *mdx* as compared to control fibres. This does not favour the hypothesis according to which muscle necrosis in dystrophic animals is due to intracellular calcium overload (Turner *et al.* 1988). Furthermore, our data suggest that, as mice get older, the resting $[Ca^{2+}]_i$ may even be regulated at a significantly lower level in *mdx* fibres than in control ones. We wish, however, to be careful with such assessments, as well as with comparison of the present results with previously published data. First, in the present work, isolated muscle fibres were partially insulated with silicone and bathed in the presence of a rather 'exotic' external solution. The possibility cannot be excluded that these conditions affect the mechanisms involved in resting $[Ca^{2+}]_i$ regulation so as to hinder expression of a potential defect in *mdx* fibres. Second, as suggested by Denetclaw *et al.* (1994) and Pressmar *et al.* (1994), one cannot rule out the possibility that enzymatic dissociation of the muscles may have selectively killed a population of fibres with high resting $[Ca^{2+}]_i$. Within the present study, an additional step of fibre selection was implicitly performed since we only worked with fibres that exhibited normal shape and regular striation spacing, as it would have made no sense to include spoiled-looking fibres, some of which can always be detected in a batch of either control or *mdx* dissociated muscle fibres. Thus, data presented here refer strictly to measurements performed on healthy-looking fibres that were only distinguished by the fact that they were obtained from either control or *mdx* muscles. Within these limits, dystrophin-deficient muscle fibres did not exhibit an average elevated resting $[Ca^{2+}]_i$ level. Of course, it still remains possible that a high $[Ca^{2+}]$ stays confined within a restricted subsarcolemmal area of the *mdx* cells (Turner *et al.* 1991), so that it would remain undetectable from our global fluorescence measurements. Alternatively, and as already suggested by Tutdibi *et al.* (1999), the reported increased membrane permeability for Ca^{2+} in *mdx* cells may actually be well compensated by efficient myoplasmic Ca^{2+} extrusion mechanisms. From our data, it would, however, be hard to speculate so as to favour either the occurrence of such efficient compensation mechanisms, or the possibility that the small *mdx* fibres used in the present study remain unaffected by the absence of dystrophin in terms of intracellular calcium homeostasis. Concerning the low level of resting $[Ca^{2+}]_i$ in muscle fibres from the oldest *mdx* mice tested in our study, it is tempting to relate it to the known age dependency of the *mdx* muscle physiopathological pattern. For instance, data from DiMario *et al.* (1991) showed that, in the *mdx* mouse limb skeletal muscles, cycles of degeneration–regeneration are almost completed by ∼15–20 weeks of age, suggesting that regenerated muscle fibres have an escape mechanism that provides normalised function. Along this line, we could then speculate that resting $[Ca^{2+}]_i$ may somehow become down regulated as a result of a developmental change in *mdx* muscles. In any case, our results at least re-emphasise the potential importance of the age of the animals when studying the *mdx* muscle model.

$[Ca^{2+}]_i$ transients evoked by membrane depolarization

Indo-1 calcium transients elicited by controlled membrane depolarizations looked very much alike in control and *mdx* muscle fibres. In other words, there was hardly any obvious way we could distinguish a control from an *mdx* fibre on the basis of the qualitative features of the signals. This, together with the general trend of quantitative results which demonstrated no dramatic alteration in terms of the voltage dependence of $[Ca^{2+}]_i$ changes, absolute values of peak $[Ca^{2+}]_i$ and kinetics of $[Ca^{2+}]_i$ decay, indicates that, if *mdx* muscles fibres indeed suffer from a deficient $[Ca^{2+}]_i$ regulation, it definitely does not impair their capacity to develop and remove large myoplasmic Ca^{2+} elevations. We are aware of the uncertainties in the results due to the limits inherent to the $[Ca^{2+}]_i$ detection method. In particular, strong indo-1 saturation clearly did not allow accurate resolution of peak $[Ca^{2+}]_i$ transients in the upper micromolar range. Furthermore, the $[Ca^{2+}]_i$ transients presented here were not corrected for indo-1 binding kinetics. Within this work, kinetic correction was, however, not so critical inasmuch as our main goal was to compare two groups of fibres, so any difference or absence of difference that would appear between the two groups in non-corrected records should also do so after correction. It should, though, be kept in mind that the values for the time constant of $[Ca^{2+}]_i$ decay reported here certainly underestimate the actual rates of decay (see for instance Hollingworth *et al.* 1996). Both of these problems would have been circumvented by the use of a lower affinity dye, but as a drawback the resting $[Ca^{2+}]_i$ would then not have been determined.

Interestingly, analysis of the $[Ca^{2+}]_i$ decay rate revealed that the mean time constant after a 5 ms duration pulse at 0 mV was significantly elevated in *mdx* fibres as compared to control ones. This result can be compared to some previous observations performed on calcium transients elicited by brief field stimulation pulses: Turner *et al.* (1988, 1991) reported that the half-time of $[Ca^{2+}]_i$ decay was larger in

mdx than in control fibres. Also, Tutdibi *et al.* (1999) reported that the fraction of *mdx* fibres that exhibited large decay time constants of fura-2 fluorescence ratio transients was higher in *mdx* than in control fibres. In contrast, Head (1993) showed that the half-decay time of an $[Ca^{2+}]_i$ transient in response to a single action potential was identical in control and *mdx* fibres. Although results from Head (1993) are definitely more convincing as they combined simultaneous measurement of $[Ca^{2+}]_i$ and membrane potential, the reason for the disagreement was and still remains obscure. In our hands, the rate of $[Ca^{2+}]_i$ decay after a short pulse was slower in *mdx* than in control fibres irrespective of the level of resting $[Ca^{2+}]_i$, which disagrees with the slow decay being a consequence of an elevated resting $[Ca^{2+}]_i$ (Turner *et al.* 1991). Furthermore, the observed difference in the decay rate between control and *mdx* fibres after a 5 ms duration pulse could have resulted from a higher peak $[Ca^{2+}]_i$ in *mdx* fibres, since this would be expected to produce a higher level of saturation of intrinsic Ca^{2+} buffers and a consequent slower rate of calcium removal. However, this was obviously not the case, since in one series of measurements, the mean peak $[Ca^{2+}]_i$ after a 5 ms pulse was not significantly different in control and *mdx* fibres (see Fig. 4*B*), while in the other series of measurements, the mean peak $[Ca^{2+}]_i$ after a 5 ms pulse was significantly lower in the *mdx* fibres than in the control ones (see Fig. 7*B*).

The possibility that *mdx* fibres suffer from impaired myoplasmic calcium removal mechanisms has previously been raised. For instance, it was reported that the maximum velocity of sarcoplasmic reticulum (SR) Ca^{2+} uptake is lower in *mdx* than in control fibres (Kargacin & Kargacin, 1996). On the other hand, the total parvalbumin content seems to be normal (Anderson *et al.* 1988; Gillis, 1996). A reduced rate of SR calcium uptake should presumably produce a low overall rate of myoplasmic calcium removal whatever the duration of the depolarizing pulse (see for instance Jacquemond & Schneider, 1992), which was clearly not the case under our conditions.

In conclusion, under our experimental conditions, no gross alteration of macroscopic $[Ca^{2+}]_i$ handling could be detected in *mdx* as compared to control skeletal muscle fibres. The reduced rate of $[Ca^{2+}]_i$ decay that was observed after short depolarizing pulses may be speculated to be indicative of a subtle difference, of unclear origin, in $[Ca^{2+}]_i$ regulation between control and *mdx* fibres. However, further investigations will be required in order to confirm this observation and reveal the underlying mechanism. From a more general point of view, the overall significance of our findings is of course limited, as it is known that the aetiology of the dystrophic process is much milder in the *mdx* model than in DMD patients. It could, however, still be suggested that in the *mdx* mouse the presence of healthy muscle fibres that regulate intracellular calcium well, is somehow related to the milder physiopathological consequences of the disease.

Anderson, J. E., Bressler, B. H. & Ovalle, W. K. (1988). Functional regeneration in the hindlimb skeletal muscle of the mdx mouse. *Journal of Muscle Research and Cell Motility* **9**, 499–515.

Bakker, A. J., Head, S. I., Williams, D. A. & Stephenson, D. G. (1993). Ca^{2+} levels in myotubes grown from the skeletal muscle of dystrophic (*mdx*) and normal mice. *Journal of Physiology* **460**, 1–13.

Berthier, C., Amsellem, J. & Blaineau, S. (1995). Visualization of the subsarcolemmal cytoskeleton network of mouse skeletal muscle cells by en face views and application to immunoelectron localization of dystrophin. *Journal of Muscle Research and Cell Motility* **16**, 553–566.

Bulfield, G., Siller, W. G., Wight, P. A. & Moore, K. J. (1984). X chromosome-linked muscular dystrophy (*mdx*) in the mouse. *Proceedings of the National Academy of Sciences of the USA* **81**, 1189–1192.

Carnwath, J. W. & Shotton, D. M. (1987). Muscular dystrophy in the mdx mouse: histopathology of the soleus and extensor digitorum longus muscles. *Journal of the Neurological Sciences* **80**, 39–54.

Collet, C., Allard, B., Tourneur, Y., Rougier, O. & Jacquemond, V. (1999). Indo-1 calcium signals in skeletal muscle fibers from normal and mdx mice. *Biophysical Journal* **76**, A298.

Csernoch, L., Bernengo, J. C., Szentesi, P. & Jacquemond, V. (1998). Measurements of intracellular Mg^{2+} concentration in mouse skeletal muscle fibers with the fluorescent indicator mag-indo-1. *Biophysical Journal* **75**, 957–967.

Denetclaw, W. F., Hopf, F. W., Cox, G. A., Chamberlain, J. S. & Steinhardt, R. A. (1994). Myotubes from transgenic *mdx* mice expressing full-length dystrophin show normal calcium regulation. *Molecular Biology of the Cell* **5**, 1159–1167.

DiMario, J. X., Uzman, A. & Strohman, R. C. (1991). Fiber regeneration is not persistent in dystrophic (MDX) mouse skeletal muscle. *Developmental Biology* **148**, 314–321.

Fong, P., Turner, P. R., Denetclaw, W. F. & Steinhardt, R. A. (1990). Increased activity of calcium leak channels in myotubes of Duchenne human and *mdx* mouse origin. *Science* **250**, 673–676.

Gailly, P., Boland, B., Himpens, B., Casteels, R. & Gillis, J. M. (1993). Critical evaluation of cytosolic calcium determination in resting muscle fibres from normal and dystrophic (mdx) mice. *Cell Calcium* **14**, 473–483.

Gillis, J. M. (1996). Membrane abnormalities and Ca homeostasis in muscles of the mdx mouse, an animal model of the Duchenne muscular dystrophy: a review. *Acta Physiologica Scandinavica* **156**, 397–406.

Grynkiewicz, G., Poenie, M. & Tsien, R. Y. (1985). A new generation of Ca^{2+} indicators with greatly improved fluorescence properties. *Journal of Biological Chemistry* **260**, 3440–3450.

Head, S. I. (1993). Membrane potential, resting calcium and calcium transients in isolated muscle fibres from normal and dystrophic mice. *Journal of Physiology* **469**, 11–19.

Hoffman, E. P., Knudson, C. M., Campbell, K. P. & Kunkel, L. M. (1987). Subcellular fractionation of dystrophin to the triads of skeletal muscle. *Nature* **330**, 754–758.

Hollingworth, S., Zaho, M. & Baylor, S. M. (1996). The amplitude and time course of the myoplasmic free $[Ca^{2+}]$ transient in fast-twitch fibers of mouse muscle. *Biophysical Journal* **108**, 455–469.

Hopf, F. W., Turner, P. R., Denetclaw, W. F., Reddy, P. & Steinhardt, R. A. (1996). A critical evaluation of resting intracellular free calcium regulation in dystrophic *mdx* muscle. *American Journal of Physiology* **271**, C1325–1339.

Jacquemond, V. (1997). Indo-1 fluorescence signals elicited by membrane depolarization in enzymatically isolated mouse skeletal muscle fibers. *Biophysical Journal* **73**, 920–928.

Jacquemond, V. & Schneider, M. F. (1992). Effects of low myoplasmic Mg^{2+} on calcium binding by parvalbumin and calcium uptake by the sarcoplasmic reticulum in frog skeletal muscle. *Journal of General Physiology* **100**, 115–135.

Kargacin, M. E. & Kargacin, G. J. (1996). The sarcoplasmic reticulum calcium pump is functionally altered in dystrophic muscle. *Biochimica et Biophysica Acta* **1290**, 4–8.

Klein, M. G., Simon, B. J., Szucs, G. & Schneider, M. F. (1988). Simultaneous recording of calcium transients in skeletal muscle using high- and low-affinity calcium indicators. *Biophysical Journal* **53**, 971–988.

Leijendekker, W. J., Passaquin, A. C., Metzinger, L. & Rüegg, U. T. (1996). Regulation of cytosolic calcium in skeletal muscle cells of the mdx mouse under conditions of stress. *British Journal of Pharmacology* **118**, 611–616.

Melzer, W., Herrmann-Frank, A. & Lüttgau, H. C. (1995). The role of Ca^{2+} ions in excitation-contraction coupling of skeletal muscle fibres. *Biochimica et Biophysica Acta* **1241**, 59–116.

Pressmar, J., Brinkmeier, H., Seewald, M. J., Naumann, T. & Rüdel R. (1994). Intracellular Ca^{2+} concentrations are not elevated in resting cultured muscle from Duchenne (DMD) patients and in MDX mouse muscle fibres. *Pflügers Archiv* **426**, 499–505.

Turner, P. R., Fong, P., Denetclaw, W. F. & Steinhardt R. A. (1991). Increased calcium influx in dystrophic muscle. *Journal of Cell Biology* **115**, 1701–1712.

Turner, P. R., Westwood, T., Regen, C. M. & Steinhardt, R. A. (1988). Increased protein degradation results from elevated free calcium levels found in muscle from mdx mice. *Nature* **335**, 735–738.

Tutdibi, O., Brinkmeier, H., Rüdel, R. & Föhr, K. J. (1999). Increased calcium entry into dystrophin-deficient muscle fibres of MDX and ADR-MDX mice is reduced by ion channel blockers. *Journal of Physiology* **515**, 859–868.

Watkins, S. C., Hoffman, E. P., Slayter, H. S. & Kunkel, L. M. (1988). Immunoelectron microscopic localization of dystrophin in myofibres. *Nature* **333**, 863–866.

Acknowledgements

This study was supported by the Centre National de la Recherche Scientifique (CNRS), the Université Claude Bernard and by a grant from the Association Française contre les Myopathies (AFM).

We thank Drs Carlos Ojeda and Oger Rougier for helpful discussion and for critically reading the manuscript.

Corresponding author

V. Jacquemond: Laboratoire de Physiologie des Eléments Excitables, CNRS UMR 5578, Université Claude Bernard, 43 boulevard du 11 Novembre 1918, Bâtiment 401B, 69622 Villeurbanne Cedex, France.

Email: vincent.jacquemond@physio.univ-lyon1.fr